ISSN 1070-3632, Russian Journal of General Chemistry, 2014, Vol. 84, No. 7, pp. 1450–1457. © Pleiades Publishing, Ltd., 2014.

Synthesis of the 2,3,4-Triacetyl-1,6-dideoxy-L-mannose and Tetracetyl-3,6-dideoxy-L-mannitol and the Study of the Reaction Mechanism by Molecular Modeling[1]

A. E. Bañuelos-Hernández[a] and J. A. Mendoza-Espinoza[b]

[a] *Departamento de Farmacología,*
Centro de Investigación y de Estudios Avanzados del Instituto Politécnico Nacional (CINVESTAV IPN), México D.F.
e-mail: amendozaespinoza@gmail.com; josealberto.mendoza@uacm.edu.mx

[b] *Academia de Biología Humana, Colegio de Ciencia y Humanidades,*
Universidad Autónoma de la Ciudad de México (UACM), México D.F. Cátedra Amelia Sámano Bishop,
Universidad Autónoma Metropolita-Iztapalapa (UAM-Izp)

Received June 26, 2014

Abstract—The carbohydrate compounds have interesting stereochemical properties and can be used as chiral building blocks in the production of more complex derivatives. L-Rhamnose has been reported to participate in the synthesis of cytotoxic α-pyrones owing to the stereochemistry of the hydroxy groups. To study the conformational properties of acetyl derivatives of L-rhamnose, it was tosylated with the subsequent reduction and acetylation. These series of reactions produced an interesting mixture of poly-acetylated compounds. The mixture was separated by HPLC, characterized by 1D and 2D NMR techniques and compared with models obtained on DFT/B3LYP/DGDZVP theory level of calculation, taking into account the effect of pyridine as solvent in the transformation of this carbohydrate. The results show a mixture of three pyranoside products with tosyl group in positions 2, 3, and 4. These latter compounds after reduction with aluminum hydride and acetylation yielded two main products, one triacetate pyranoside and an open-chain mannositol tretraacetate.

Keywords: L-rhamnose, molecular modeling, conformational analysis, reaction mechanism

DOI: 10.1134/S1070363214070342

INTRODUCTION

Cancer disease results from abnormal proliferation of any of the different kinds of cells in the human body. The treatments consist in several techniques; one of these treatments is the chemotherapy [1]. The natural products found in vegetal species with anti-cancer activity are related to topaclitaxel [2], disco-dermolide [3], vinorelbine [4], colchicine [5], pironetin [6]. A common characteristic of this type of natural compounds are the complicated chemical structures with the presence of several chiral centers. For this reason, in the total synthesis of natural products are used small fragments considered as "construction blocks." These small fragments contain the same stereochemical configuration of the natural product and can be functionalised.

For the synthesis of several natural products, the construction blocks can be obtained from monomeric carbohydrates like glucose, rhamnose, fucose, or galactose, example of this is the total synthesis of discodermolide and spicigerolide [7], in this latter, the L-rhamnose is used as a construction block [8]. For this reason, it is necessary to study the reaction mechanism of carbohydrate monomers in several reaction conditions. The molecular flexibility of these compounds implies a large number of conformations, and then the search for the optimal conformer that leads a reaction is more complicated. The conforma-tional analysis and reaction mechanisms of flexible compounds can be studded using molecular modeling described in the previous papers as:

(1) Determination of the stereochemical centres of hypurticin, spicigerolide, and hyptolide, established by comparison of the proton-proton coupling constants calculated by molecular modeling versus the experi-mental spectrum [9].

(2) Reactivity studies of diphenyl-dithioacetals. In this study the differences in the reactivity of two

[1] The text was submitted by the authors in English.

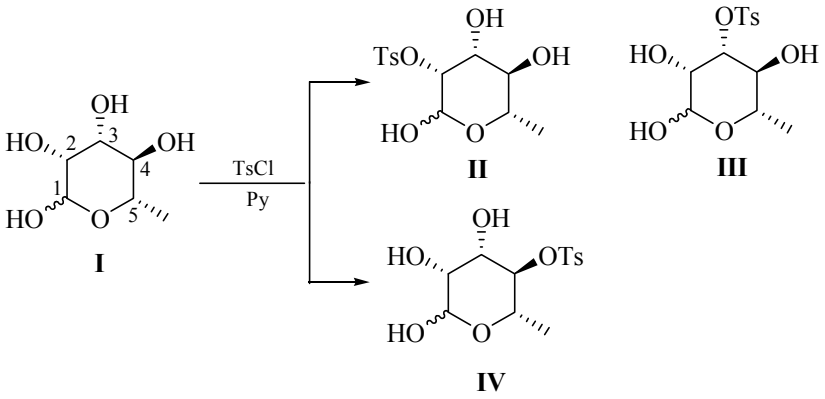

Fig. 1. Tosylation scheme of L-rhamnose (**I**) yielding a mixture of tosylated products in different positions of the pyranoside hydroxy groups.

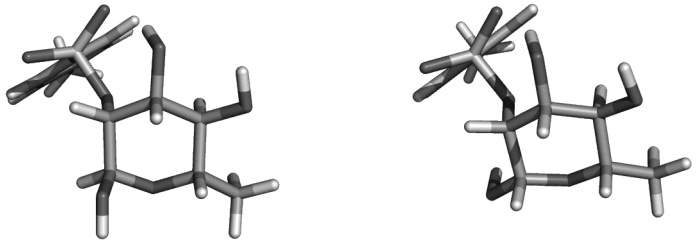

1*R*-**II**	1*S*-**II**
$\Delta G_{(\text{in vacuo})}$ = –897816.682 kcal/mol	$\Delta G_{(\text{in vacuo})}$ = –897814.949 kcal/mol
$\Delta G_{(\text{pyridine})}$ = –897817.894 kcal/mol	$\Delta G_{(\text{pyridine})}$ = –897817.164 kcal/mol

Fig. 2. Comparison of the B3LYP/DGDZVP energies of the minimum energy confomers of compound **II**. The most stable conformer is the anomer 1*R* in the calculation in vacuo as well as in pyridine solution.

diastereomers using molecular modeling was determined [10].

The aim of this work was the synthesis of tetracetyl-3,6-dideoxy-mannitolas a construction block, the conformational analysis of the precursors and the study of the reaction mechanism by molecular modeling. These results can provide information on the synthesis of more complex structures, and the method described herein can be employed for the conformational analysis of flexible fragments.

RESULTS AND DISCUSSION

The tosylation of L-Rhamnose (**I**) in pyridine resulted in the formation of a mixture of three pyranoside products in positions C-2, C-3 and C-3 of the pyran ring (**II**, **III,** and **IV**, respectively). The products **III** and **IV** were isolated by HPLC, however **II** was not isolated in a pure form because it suffer a transesterification reaction at room temperature and transformed into compound **III** spontaneously (Fig. 1).

In order to explain the transformation of compound **II** into **III**, the ΔG of each compound were calculated and compared. The conformer distribution was calculated by Monte Carlo–MMFF, single point calculations at posteriori with DFT/B3LYP/6-31G(d), then optimized with B3LYP/DGDZVP. The 1D and 2D NMR spectra with *J* couplings of the mixture were used to the assessment of the experimental conformation. Thus, as the presence of an anomeric centre in the position 1 of the cyclic molecules, the modeling was calculated for the 1*R* and 1*S* compounds. The calculations were performed in vacuo or in pyridine using Onsager method. The minimum energy conformers are shown in Fig. 2.

Compound **III** was isolated and characterized by HPLC and NMR. The calculations were performed equally as for compound **II**. Same as above, the reaction produced the 1*R* and 1*S* mixture, the calculations of ΔG were performed for both cases (Fig. 3).

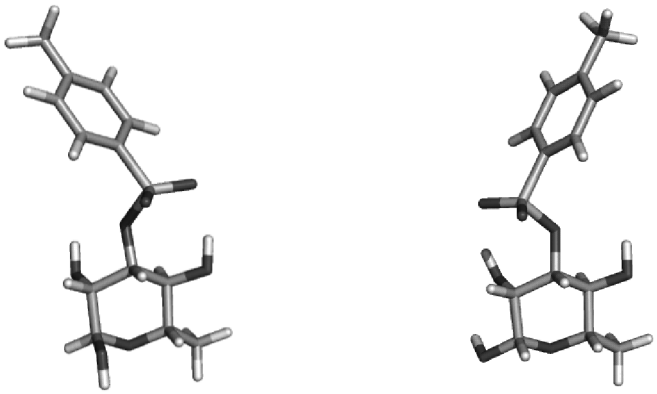

1*R*-**III**
$\Delta G_{(\text{in vacuo})}$ = –897815.754 kcal/mol
$\Delta G_{(\text{pyridine})}$ = –897817.938 kcal/mol

1*S*-**III**
$\Delta G_{(\text{in vacuo})}$ = –897815.422 kcal/mol
$\Delta G_{(\text{pyridine})}$ = –897818.707 kcal/mol

Fig. 3. Comparison of the B3LYP/DGDZVP energies of the minimum energy conformers of compound **III**. The most stable conformer is the anomer 1*S*, both in vacuo and in pyridine solution model.

The comparison of energies calculated in vacuo shows that the 1*R* anomer of **II** is a low energy state, however the energies of the 1*R* and 1*S* anomers of **III** are in half way of the anomer 1*S* of **II**. Comparing the solvation modelled systems of these compounds, the calculated energies show that both anomers of compound **III** are more stable than those of **II**, the energy state of the reaction product **II** tends toward the formation of the mixture of *R* and *S* products of **III**. The examination of all the energies of all models shows that Δ*G* calculated in pyridine for the anomer *S* of compound **III** is the most stable. With these values of Δ*G* the transesterification of compound **II** to yield the substance **III** can be understood. Geometrically, the spatial arrangement of the sulfur in the sulfone group in position 2 and –OH in position 3 in all conformers of compound **II** led to an intramolecular nucleophilic attack (a distance of 3.45 Å in the lowest energy conformer), the compound **III** as the product of this attack is a more stable conformation in pyridine as solvent. The interatomic distance between the –OH in position 2 and the sulfur atom is longer (4.39 Å in the lowest energy conformer) preventing the reverse reaction leading the equilibrium from substance **II** to substance **III**.

To prove the conformation of the most stable conformer of **III**, the experimental ^{1}H–^{1}H *vicinal* coupling constants of the pyran ring were compared to the conformer group weighted with the Boltzmann distribution with the Δ*G* values calculated by B3LYP/DGDZVP. Due to the solubility of the compounds, the experimental NMR spectroscopy was performed in DMSO-d_6 as solvent, to compensate this condition the whole conformer distribution was calculated with the Onsager method using the dielectrical constant for DMSO. The three most stable conformers of the anomer *S* of **III** in DMSO are shown in Fig. 4.

The conformer distributions in DMSO and in pyridine are very similar (Table 1), thus, the calculations of the ^{1}H–^{1}H *vicinal* coupling constants are an accurate reflection of the distribution occurring in pyridine. The theoretical ^{1}H–^{1}H coupling constants of the conformer distribution of compound **III** (Table 2),

Table 1. Comparison between the Δ*G* energies and Boltzmann abundances of the conformations of compound **III** in different solvents

Conformer	Δ*G*, kcal/mol		
	in vacuo	pyridine	DMSO
III-1	−897815.363 (30.4%)	−897818.707 (73.3%)	−897819.160 (75.5%)
III-2	−897815.422 (33.6%)	−897818.082 (25.5%)	−897818.474 (23.7%)
III-3	−897814.432 (>6.0%)	−897816.150 (<1.0%)	−897816.351 (<0.7%)

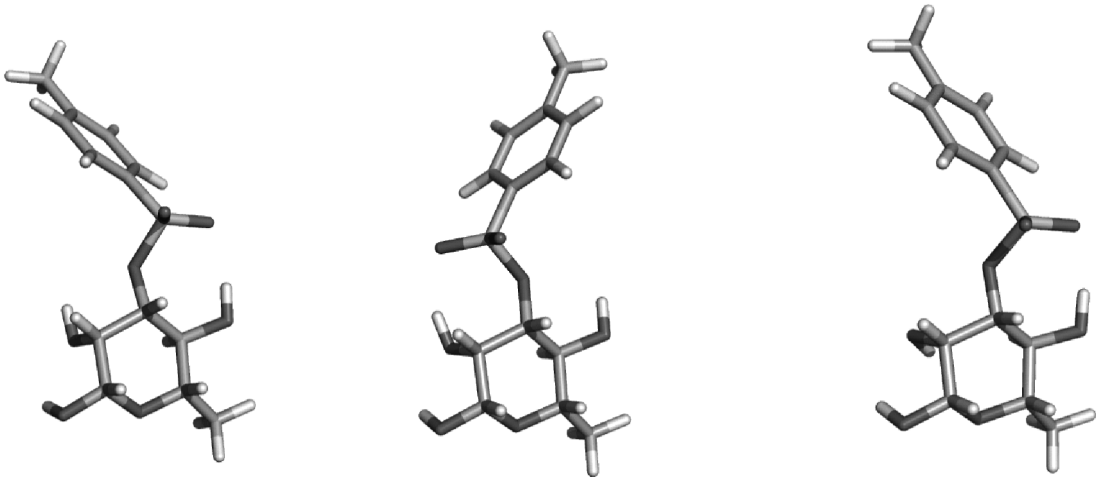

III-1
$\Delta G_{(DMSO)}$ = −897819.160 kcal/mol
(75.5%)

III-2
$\Delta G_{(DMSO)}$ = −897818.474 kcal/mol
(23.7%)

III-3
$\Delta G_{(DMSO)}$ = −897816.351 kcal/mol
(<0.7%)

Fig. 4. The most abundant conformers of **III** in theoretical distribution with DMSO as solvent, the Gibbs Energies and their abundances in percentages are shown.

fits the experimental coupling constants with a root-mean-square error of 0.68 Hz of chemical shift validating the conformational search method.

The presence of compound **II** is relevant because it participates dynamically in two elquilibria, the first as mentioned before, contributing to the formation of **III**; and the second, as a result of the reduction with $LiAlH_4$ and acetylation of the mixture of **II** and **III**, it produces triacetyl-1,6-dideoxy-mannopyranose (**V**) and an open-chain molecule of tetracetyl-3,6-dideoxy-mannitol (**VI**) as shown in Fig. 5. The generation of **VI** is readily explained by the reduction and the entrance of two hydride groups in the anomeric carbon and the electropositive center of the tosyl-based carbon of compound **III**. However, the production of compound **V** is not easily explained by the hydride entrance, as can be seen in the inversion of the chiral center in the position C-2. Compound **II** underwent in the intramolecular oxygen migration favored by the geometry, and possibly the formation of an epoxide-like intermediate **IIa**; to favour this step the geometry of the anomeric carbon shall be in the *R* form. This is supported by the calculation of the most stable conformations of substance **II** in pyridine, the anomer *R* is more stable and can lead to the formation of the epoxide-like intermediate **IIa**. It is important to mention that the existence of the *S* anomer is limited by the LeChetelier principle, because *S* anomer is less stable than *R* according to the calculation. With the introduction of the hydride, the epoxide-like compound forms the trihydroxylated substance **IIb** (Fig. 5). The pyran ring of **IIb** is not opened due to the stability of the ether functionality in highly alkaline

Table 2. Vicinal $^1H–^1H$ spin-spin coupling constants (*J*) calculated in DMSO for principal conformers of compound **III**

Conformer	*P*	$J_{1,2}$, Hz	$J_{2,3}$, Hz	$J_{3,4}$, Hz	$J_{4,5}$, Hz
III-1	0.7548	1.9	3.9	8.6	8.7
III-2	0.2371	2.6	3.8	8.7	8.9
III-3	0.0066	1.1	4.5	8.9	8.8
Theoretical *J* [a, c]		2.0	3.9	8.6	8.7
Experimental *J* [b, c]		1.8	3.3	9.5	9.5

[a] Calculated by DFT/B3LYP/DGDZVP and Onsager method. [b] Measured in 300 MHz/DMSO-d_6. [c] The root-mean-square error between the theoretical and experimental coupling constants is 0.68 Hz.

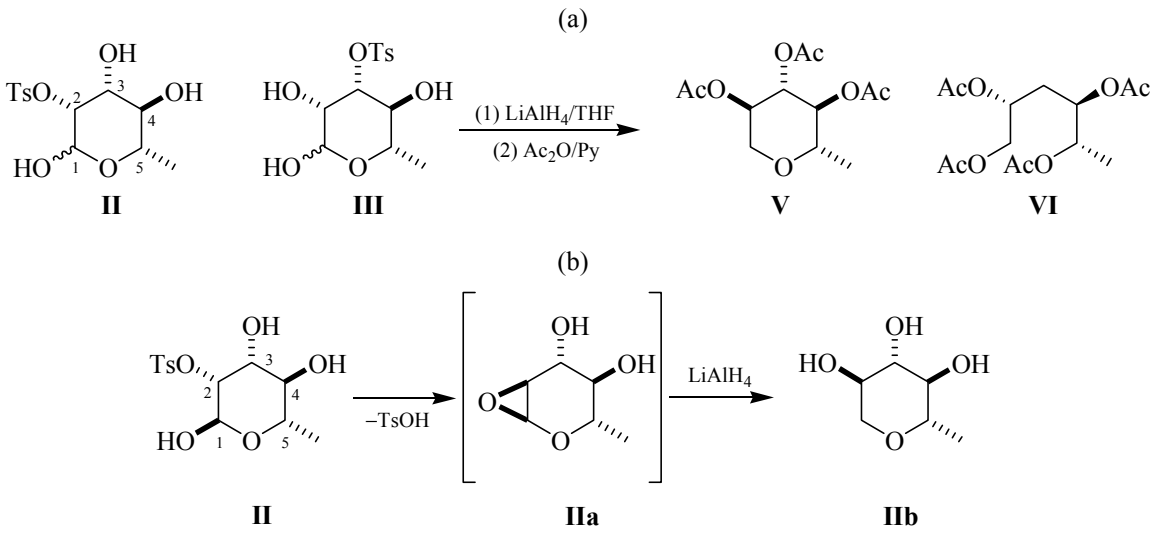

Fig. 5. Reduction and acetylation of the mixture of compound **II** and **III**; this scheme shows the triacetyl pyranoside **V** and the tetraacetyl mannoside **VI** (a). Compound **II** suffers an intramolecular nucleophilic attack (b), then produces an epoxide like intermediary (**IIa**); with the hydride entrance, the obtained compound is the trihydroxylated pyran **IIb**.

and reducing medium. Subsequently the trihydroxylated methylpyran (**IIb**) is acetylated with acetic anhydride to yield compound **V**.

Product **V** was analysed by Monte Carlo/MMFF 94 and DFT/B3LYP/DGDZVP methods. The conformer distribution of compound **V** was limited to almost one conformer (Fig. 6). The calculation of the conformer distribution was performed with the DFT methods mentioned previously using the Onsager solvation model, as the solvent used in experimental NMR was deuterochloroform ($CDCl_3$), thus, the calculation for the NMR parameters in solution was set properly. The ΔG of the models calculated in vacuo and that calculated in chloroform do not have an important difference reflected in the molar contribution in equilibrium, the lack of this difference is due the low relative permittivity of both media (defined as 1 for the vacuum and 4.7113 for chloroform at 25°C). The calculated $^1H–^1H$ coupling constant fits accordingly the experimental coupling constant measured in $CDCl_3$ with a route-mean square error of 0.48 Hz (Table 3).

EXPERIMENTAL

Molecular Modeling

The molecular modeling was carried out using the Spartan·04W software and employing the Monte Carlo method in combination with MMFF for the search of conformers [11]. The selected conformers were situated within an interval of 5 kcal/mol from the minimum energy conformer. The modeled structures inside the cut-off value of 5 kcal/mol were geometrically optimized, thermochemical and vibrational properties were calculated with the Density Functional Theory (DFT) using the method B3LYP and the basis DGDZV as implemented in the Gaussian 03W program package [12–14]. The solvation energy and the Gibbs Energy in solution were calculated employing the Onsager method [15], the molecular

Table 3. Vicinal $^1H–^1H$ spin-spin coupling constants (J) calculated for principal conformers of compound **V**

Conformer	P	$J_{1pro\text{-}R,\,1pro\text{-}S}$, Hz	$J_{1Pro\text{-}R,\,2}$, Hz	$J_{1Pro\text{-}S,\,2}$, Hz	$J_{2,3}$, Hz	$J_{3,4}$, Hz	$J_{4,5}$, Hz
V	0.9918	–11.73	5.99	10.05	9.71	9.42	9.48
Theoretical J [a, c]		–11.73	5.99	10.05	9.71	9.42	9.48
Experimental J [b, c]		–11.10	5.80	11.00	9.50	9.50	9.50

[a] Calculated by DFT/B3LYP/DGDZVP and Onsager method. [b] Measured in 300 MHz/$CDCl_3$. [c] The root-mean-square error between the theoretical and experimental coupling constants is 0.48 Hz.

volumes were calculated for each selected conformer of the distribution, then the optimization and the properties were calculated using the keyword SCRF and the parameter "DIELECTRIC" employing the values of 4.7113 for chloroform, 12.978 for pyridine, and 46.826 for dimethyl sulfoxide. To discard the conformer models of transition states, the conformers with imaginary frequencies were omitted. The participation of the conformers in the equilibrium was calculated with the Boltzmann distribution, based in the method previously described for the cases of hypurticine and hyptolide [9].

To validate the conformer distribution, the magnetic shielding tensors were calculated with the Gauge-Including Atomic Orbital (GIAO) method, followed by theoretical calculation of the total NMR Spin-Spin Coupling Constants at the B3LYP/ DGDZVP level. The $\Delta G = -RT\ln K$ equation was used to obtain the population for each conformer taking into consideration a cyclic equilibrium among the selected conformers [16-18]. Each coupling constant value was Boltzmann-weighted with the DFT population to integrate the population-averaged coupling constants [19, 20].

Preparation of the Rhamnosyl *p*-Toluensulfonates

2-Tosyl-rhamnose (II) and 3-tosyl-rhamnose (III). A solution of L-rhamnose (**I**) (5 g) in pyridine (5 mL) was treated with *p*-toluensulfonyl chloride (10 g) at room temperature during 72 h. Then the reaction mixture was extracted with ethyl acetate, washed with 10% HCl, neutralized with $KHCO_3$ and salted out with 1% NaCl. The reaction yielded a mixture of tosylated compounds, the mixture was purified in silica gel column and eluted with dichloroethane–methanol (97 : 3), the product mixture of **II** and **III** appeared as a white solid, this mixture was resolved by High Performance Liquid Chromatography (HPLC), semi-preparative silica column, mobile phase ethylacetate–hexane (9 : 1), flow rate 1 mL/min reaching a pressure of 450 psi. The chromatogram shows two main peaks corresponding to compounds **II** and **III**. The major peak corresponded to the pure compound **III**; the minor peak belongs to compound **II**, which isomerizes via tosyltransesterification to substance **III** [21]. mp. 125–135°C, R_f = 0.4 (CH_2Cl_2–MeOH, 9 : 1). ORD (*c* = = 0.34, MeOH) $[\alpha]_{589}$ = +0.9°, $[\alpha]_{578}$ = +1.2°, $[\alpha]_{546}$ = +1.5°, $[\alpha]_{436}$ = +2.1°, $[\alpha]_{356}$ = +3.2°. IR (KBr), ν_{max}, cm^{-1}: 3624 (OH), 3524 (OH), 3390 (OH), 1930 (di-susbtituted *p*-aromatic), 1356 (SO_2), 1174 (SO_2), 1038 (C–O). UV (EtOH), λ_{max}, nm (log ε) 227 (4.25), 257 (2.98), 262 (2.98), 2.68 (2.98), 273 (280). ^{1}H NMR spectrum (300 MHz, DMSO-d_6), δ, ppm: 7.77 d (2H $J_{2'\text{-}3'}J_{5'\text{-}6'}$ = 8.4 Hz, $H^{2'}$, $H^{6'}$), 7.41 d (2H, $J_{2'\text{-}3'}J_{5'\text{-}6'}$ = 8.4 Hz, $H^{3'}$, $H^{5'}$), 6.46 d (1H, $J_{1\text{-}OH^1}$ = 4.0 Hz, OH^1), 5.19 d (1H, $J_{4\text{-}OH^4}$ = 6.6 Hz, OH^4), 5.17 (1H, d, $J_{2\text{-}OH^2}$ = 7.0 Hz, OH^2), 4.76 d.d (1H, $J_{1\text{-}OH^1}$ = 4.0 Hz, $J_{1\text{-}2}$ = 1.8 Hz, H^1), 4.40 d.d (1H, $J_{2\text{-}3}$ = 3.3 Hz, $J_{3\text{-}4}$ = 9.5 Hz, H^3), 3.66 d.d.d (1H, $J_{1\text{-}2}$ = 1.8 Hz, $J_{2\text{-}3}$ = 3.3 Hz, $J_{2\text{-}OH^2}$ = 7.0 Hz, H^2), 3.59 d.q (1H, $J_{4\text{-}5}$ = 9.5, $J_{5\text{-}6}$ = 6.2 Hz, H^5), 3.38 d.t (1H, $J_{3\text{-}4}$ = 9.5 Hz, $J_{4\text{-}OH^4}$ = 6.6 Hz, $J_{4\text{-}5}$ = 9.5, H^4), 2.41 s (3H, $Me^{7'}$), 1.09 d (3H, $J_{5\text{-}6}$ = 6.2 Hz, Me^6). ^{13}C NMR spectrum (75.4 MHz, DMSO-d_6), δ, ppm: 144.3 (1C, $C^{1'}$), 133.9 (1C, $C^{4'}$), 129.7 (2C, $C^{2'}$, $C^{6'}$), 127.7 (2C, $C^{3'}$, $C^{5'}$), 93.9 (1C, C^1), 82.8 (1C, C^3), 69.6 (1C, C^2), 68.9 (1C, C^4), 68.0 (1C, C^5), 21.1 (1C, $C^{7'}$), 17.9 (1C, C^6). EM FAB$^+$ *m/z* 319 $[M + H]^+$ (10), 307 (80), 301 (70), 289 (50), 154 (100), 136 (95), 107 (62), 89 (51), 77 (43).

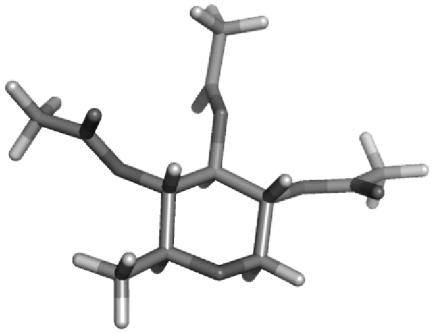

ΔG_{CHCl_3} = 624137.569 (99.18%)

Fig. 6. The most stable conformer of **V** in theoretical distribution with $CHCl_3$ as solvent, the Gibbs Energy and the abundance in percentage is shown.

4-Tosyl-rhamnose (IV). From the remaining fractions of the chromatography of the previous section a white solid was isolated, the yield was approximately 1 mg (>1%), R_f = 0.4 (CH_2Cl_2–MeOH, 9 : 1). ^{1}H NMR spectrum (300 MHz, DMSO-d_6), δ, ppm: 7.81 d (2H, $J_{2'\text{-}3}$, $J_{5'\text{-}6'}$ = 8.3 Hz, $H^{2'}$, $H^{6'}$), 7.42 d (2H, $J_{2'\text{-}3}$, $J_{5'\text{-}6'}$ = 8.3 Hz, $H^{3'}$, $H^{5'}$), 6.48 d (1H, $J_{1\text{-}OH^1}$ = 4.4 Hz, OH^1), 5.04 d (1H, $J_{2\text{-}OH^2}$ = 4.4 Hz, OH^2), 4.82 d.d (1H, $J_{1\text{-}2}$ = 1.6 Hz, $J_{1\text{-}OH^1}$ = 4.4 Hz, H^1), 4.67 d (1H, $J_{3\text{-}OH^3}$ = 7.3 Hz, OH^3), 4.44 t (1H, $J_{3\text{-}4}$ = 9.5 Hz, $J_{4\text{-}5}$ = 9.5 Hz, H^4), 3.82 d.q (1H, $J_{4\text{-}5}$ = 9.5 Hz, $J_{5\text{-}6}$ = 6.3 Hz, H^5), 3.65 d.d.d (1H, $J_{2\text{-}3}$ = 3.5 Hz, $J_{3\text{-}4}$ = 9.5 Hz, $J_{3\text{-}OH^3}$ = 7.3 Hz, H^3), 3.57 d.d.d (1H, $J_{1\text{-}2}$ = 1.6 Hz, $J_{2\text{-}3}$ = 3.5 Hz, $J_{2\text{-}OH^2}$ = 4.4 Hz, H^2), 2.40 s (3H, $Me^{7'}$), 1.08 d (3H, $J_{5\text{-}6}$ = 6.3 Hz, Me^6). ^{13}C NMR spectrum (75.4 MHz,

DMSO-d_6), δ, ppm: 144.2 (1C, $C^{1'}$), 134.6 (1C, $C^{4'}$), 129.6 (2C, $C^{2'}$, $C^{6'}$), 127.6 (2C, $C^{3'}$, $C^{5'}$), 93.7 (1C, C^1), 84.4 (1C, C^4), 72.2 (1C, C^2), 67.7 (1C, C^3), 65.1 (1C, C^5), 21.1 (1C, C^7), 17.8 (1C, C^6).

2,3,4-Triacetyl-1,6-dideoxy-L-mannose (V) and 1,2,4,5-tetraacetyl-3,6-dideoxy-L-mannitol (VI). The tosyl mixture (1 g) from the latter section (compounds **II**–**IV**), was treated with $LiAlH_4$ (1 g) in dry THF (20 mL). The reaction mixture was stirred for 30 min at room temperature, and then it was heated to reflux for 1 h. The reaction was quenched with ethanol–water, a white precipitate was formed, filtered, and dried in a Buchner funnel. The mixture was peracetylated in acetic anhydride (3 mL) and pyridine (1 mL). The mixture was washed with 10% HCl, then with saturated $KHCO_3$ and at last with water. The purification was carried out with on activated alumina column, eluted with 95 : 5 hexane–ethyl acetate yielding a 30% of **V** and a 4% of **VI**. The physical data of compound **V** is R_f = 0.4 (hexane–AcOEt, 8 : 2). ORD (c = 0.27, MeOH), $[\alpha]_{589}$ = +0.4°, $[\alpha]_{578}$ = +0.4°, $[\alpha]_{546}$ = −0.7°, $[\alpha]_{436}$ = −1.5°, $[\alpha]_{365}$ = −3.3°. IR (MeOH), ν_{max}, cm^{-1}: 1744 (C=O), 1064 (C−O), 1034 (C−O). ^1H NMR spectrum (300 Hz, $CDCl_3$), δ, ppm: 5.14 t (1H, $J_{3\text{-}4}$ = 9.5 Hz, $J_{2\text{-}3}$ = 9.5 Hz, H^3), 4.97 d.d.d (1H, $J_{1\alpha\text{-}2}$ = 5.8 Hz, $J_{1\beta-2}$ = 11.0 Hz, $J_{2\text{-}3}$ = 9.5 Hz, H^2), 4.76 t (1H, $J_{4\text{-}5}$ = 9.5 Hz, $J_{5\text{-}6}$ = 9.5 Hz, H^4), 4.06 d.d (1H, $J_{1\alpha-1\beta}$ = 11.1, Hz, $J_{1\alpha\text{-}2}$ = 5.8 Hz, $H^1{}_\alpha$), 3.45 d.q (1H, $J_{4\text{-}5}$ = 9.5 Hz, $J_{5\text{-}6}$ = 6.3 Hz, H^5), 3.26 d.d (1H, $J_{1\alpha-1\beta}$ = 11.1 Hz, $J_{1\beta-2}$ = 11.0 Hz, $H^1{}_\beta$), 2.04 s (3H, OAc), 2.02 s (3H, OAc), 2.02 s (3H, OAc), 1.20 d (3H, $J_{5\text{-}6}$ = 6.3 Hz, Me^6). ^{13}C NMR spectrum (75.4 MHz, $CDCl_3$), 170.5 (OAc), 169.9 (OAc), 169.8 (OAc), 74.7 (1C, C^5), 73.7 (1C, C^3), 73.5 (1C, C^4), 69.5 (1C, C^2), 66.7 (1C, C^1), 20.7 (OAc), 20.7 (OAc), 20.7 (OAc), 17.6 (1C, C^6). EI-EM m/z 259 $[M - CH_3]^+$ (1), 215 (3), 154 (14), 139 (5), 128 (7), 112 (38), 97 (11), 85 (16), 57 (6), 43 (100).

The physical data of compound **VI** is R_f = 0.22 (hexane–AcOEt, 8 : 2). ^1H NMR spectrum (300 MHz, $CDCl_3$), δ, ppm: 5.13 d.q (J_4^5 = 9.8 Hz, J_5^6 = 6.6 Hz, H^5), 5.05 m (2H, H^2, H^4), 4.29 d.d (1H, $J_{1a\text{-}2}$ = 3.6 Hz, $J_{1a\text{-}1b}$ = 12.0 Hz, H^1a), 4.01 d.d (1H, $J_{1b\text{-}2}$ = 5.8 Hz, $J_{1a\text{-}1b}$ = 12.0 Hz, H^{1b}), 2.08 s (3H, OAc), 2.05 s (3H, OAc), 2.05 s (3H, OAc), 2.04 s (3H, OAc), 1.85 m (2H, H^{3a}, H^{3b}), 1.22 (3H, d, J_5^6 = 6.6 Hz, H^6). The ^{13}C NMR spectrum spectrum were not measured experimentally due to the negligible sample amount. The chemical shifts were obtained by simulation in the Mestre-C program, 170.2 (OAc), 170.2 (OAc), 170.2 (OAc), 170.2 (OAc), 72.9 (1C, C^5), 70.6 (1C, C^4), 65.2 (1C, C^1), 64.4 (1C, C^2), 26.8 (1C, C^3), 21.0 (OAc), 21.0 (OAc), 21.0 (OAc), 20.7 (OAc), 15.8 (1C, C^6). EI-EM m/z 259 $[M - CH_3]^+$ (1), 215 (3), 154 (14), 139 (5), 128 (7), 112 (38), 97 (11), 85 (16), 57 (6), 43 (100)

CONCLUSIONS

The L-rhamnose **I** and mannose derivatives mentioned are important building blocks of more complex molecules with possible anticancer biological activity. The reactivity studies of these compounds can help in planning more efficient synthesis pathways. The treatment of L-rhamnose yielded a mixture of anomeric and positional isomers of tosyl compounds. According to the conformer analysis and Gibbs Energy calculation in a pyridine medium, the most stable product of the tosylation of **I** is the anomer 1*S* of compound **III**. The treatment with hydride of the mixture of **II** and **III** yielded compounds **V** and **VI**. The formation of the open-chain manoside **VI** occurs by the nucleophilic entrance of hydride in the position C^3 and in the anomeric carbon, then the subsequent acetylation yields a tetra-acetylated compound. Compound **V** originated from the not isolated intermediate **IIa**, we postulated the oxygen migration and the elimination of *p*-toluensuphonic acid, and with the entrance of hydride the intermediate **IIa** is reduced to **IIb**. It is important to remark that the liberation of *p*-toluensulphonic acid can be achieved only when the hydroxy group in C^1 and the tosyl group in C^2 are in the *anti* geometry as can be seen in the anomer 1*R* of compound **II**. Additionally the conformation of the compounds **III** and **V** were determined by theoretical methods, the coupling constants were compared between the experimental values and the calculated with B3LYP/DGDZVP method. The calculated values of coupling constants fit the experimental in both compounds calculated, as the coupling constants depend on the orientation of the hydrogens in the molecules, the models employed in this analysis are adequate and a well agree with results found in solution.

REFERENCES

1. Cooper, G.M., *The Cell, A Molecular Approach,* 2nd ed., Sinauer Associates, MA, 2000.
2. Cragg, G.M., Newman, D.J., and Snader, K.M., *J. Nat. Prod.*, 1997, vol. 60, no. 1, p. 52. DOI: 10.1021/np9604893.
3. Ruiz, C., Valderrama, K., Zea, S., and Castellanos, L., *Mar. Biotechnol.*, 2013, vol. 15, no. 5, p. 571.DOI: 10.1007/s10126-013-9510-7.

4. Giovanelli, E., Moisan, L., Comesse, S., Leroux, S., Rousseau, B., Hellier, P., Nicolas, M., and Doris, E., *Org. Biomol. Chem.*, 2013, vol. 11, p. 5885. DOI: 10.1039/C3OB41170B.
5. Frolova, L V, Magedov, I.V., Romero, A.E., Karki, M., Otero, I., Hayden, K., Evdokimov, N.M., Banuls, L.M.Y., Rastogi, S.K., Smith, W.R., Lu, S.-L., Kiss, R., Shuster, C.B., Hamel, E., Betancourt, T., Rogelj, S., and Kornienko, A., *J. Med. Chem.*, 2013, vol. 56, no. 17, p. 6886. DOI: 10.1021/jm400711t.
6. Paños, J., Díaz-Oltra, S., Sánchez-Peris, M., García-Pla, J., Murga, J., Falomir, E., Carda, M., Redondo-Horcajo, M., Díaz, J. F., Barasoain, I., and Marco, J.A., *Org. Biomol. Chem.*, 2013, vol. 11, no. 35, p. 5809. DOI: 10.1039/C3OB40854J.
7. Smith, A.B., Sugasawa, K., Atasoylu, O., Yang, C.-P.H., and Horwitz, S.B., *J. Med. Chem.*, 2011, vol. 54, no. 18, p. 6319. DOI: 10.1021/jm200692n.
8. Falomir, E., Murga, J., Ruiz, P., Carda, M., Marco, J.A., Pereda-Miranda, R., Fragoso-Serrano, M., and Cerda-García-Rojas, C.M., *J. Org. Chem.*, 2003, vol. 68, no. 14, p. 5672. DOI: 10.1021/jo034470y.
9. Mendoza-Espinoza, J.A., López-Vallejo, F., Fragoso-Serrano, M., Pereda-Miranda, R., and Cerda-García-Rojas, C.M., *J. Nat. Prod.*, 2009, vol. 72, no. 4, p. 700. DOI: 10.1021/np800447k.
10. Bañuelos-Hernandez, A.E. and Mendoza-Espinoza, J.A., *S. Afr. J. Chem*, 2012, vol. 65, p. 84.
11. Kong, J., White, C.A., Krylov, A.I., Sherrill, D., Adamson, R.D., Furlani, T.R., Lee, M.S., Lee, A.M., Gwaltney, S.R., Adams, T.R., Ochsenfeld, C., Gilbert, A.T.B., Kedziora, G.S., Rassolov, V.A., Maurice, D.R., Nair, N., Shao, Y., Besley, N.A., Maslen, P.E., Dombroski, J.P., Daschel, H., Zhang, W., Korambath, P.P., Baker, J., Byrd, E.F.C., Van Voorhis, T., Oumi, M., Hirata, S., Hsu, C.-P., Ishikawa, N., Florian, J., Warshel, A., Johnson, B.G., Gill, P.M.W., Head-Gordon, M., and Pople, J.A., *J. Comput. Chem.*, 2000, vol. 21, no. 16, p. 1532 .DOI: 10.1002/1096-987X(200012)21.
12. Godbout, N., Salahub, D.R., Andzelm, J., and Wimmer, E., *Can. J. Chem.*, 1992, vol. 70, no. 2, p. 560. DOI:10.1139/v92-079.
13. Andzelm, J. and Wimmer, E., *J. Chem. Phys.*, 1992, vol. 96, no. 2, p. 1280. DOI:10.1063/1.462165
14. Frisch, M.J., Trucks, G.W., Schlegel, H.B., Scuseria, G.E., Robb, M.A., Cheeseman, J.R., Montgomery, Jr., J.A., Vreven, T., Kudin, K.N., Burant, J.C., Millam, J.M., Iyengar, S.S., Tomasi, J., Barone, V., Mennucci, B., Cossi, M., Scalmani, G., Rega, N., Peterson, G.A., Nakatsuji, H., Hada, M., Ehara, M., Toyota, K., Fukuda, R., Hasegawa, J., Ishida, M., Nakajima, T., Honda, Y., Kitao, O., Nakai, H., Klene, M., Li, X., Knox, J.E., Hratchian, H.P., Cross, J.B., Bakken, V., Adamo, C., Jaramillo, J., Gomperts, R., Stratmann, R.E., Yazyev, O., Austin, A.J., Cammi, R., Pomelli, C., Ochterski, J.W., Ayala, P. Y., Morokuma, K., Voth, G. A., Salvador, P., Dannenberg, J. J., Zakrzewski, V. G., Dapprich, S., Daniels, A.D., Strain, M.C., Farkas, O., Malick, D.K., Rabuck, A.D., Raghavachari, K., Foresman, J.B., Ortiz, J.V., Cui, Q., Baboul, A.G., Clifford, S., Cioslowski, J.B., Liu, G., Liashenko, A., Piskorz, P., Komaromi, I., Martin, R.L., Fox, D.J., Keith, T., Al-Laham, M.A., Peng, C.Y., Nanayakkara, A.M.C., Gill, P.M.W., Johnson, B., Chen, W., Wong, M.W., Gonzalez, C., and Pople, J.A., *Gaussian 03 Program,* Gaussian, Inc., Wallingford CT, 2004.
15. Onsager, L., *J. Am. Chem. Soc.*, 1936, vol. 58, no. 8, p. 1486. DOI: 10.1021/ja01299a050.
16. López-Vallejo, F., Fragoso-Serrano, M., Suárez-Ortiz, G.A., Hernández-Rojas, A.C., Cerda-García-Rojas, C.M., and Pereda-Miranda, R., *J. Org. Chem.*, 2011, vol. 76, no. 15, p. 6057. DOI: 10.1021/jo200637g.
17. Smith, S.G. and Goodman, J.M., *J. Am. Chem. Soc.*, 2010, vol. 132, no. 37, p. 12946. DOI: 10.1021/ja105035r.
18. Stephens, P.J., Aamouche, A., Devlin, F.J., Superchi, S., Donnoli, M.I., and Rosini, C., *J. Org. Chem.*, 2001, vol. 66, no. 11, p. 3671. DOI: 10.1021/jo001403k.
19. Peralta, J.E., Scuseria, G.E., Cheeseman, J.R., and Frisch, M.J., *Chem. Phys. Lett.*, 2003, vol. 375, no. 5(6), p. 452. DOI: 10.1016/S0009-2614(03)00886-8.
20. Sychrovský, V., Gräfenstein, J., and Cremer, D., *J. Chem. Phys.*, 2000, vol. 113, no. 9, p. 3530. DOI: 10.1063/1.1286806.
21. Zagorevskii, V.A. and Kirsanova, Z.D., *Chem. Heterocycl. Compd.*, 1970, vol. 6, no. 3, p. 288. DOI: 10.1007/BF00471221.